CORROSION OF BORATED STAINLESS STEEL IN WATER AND HUMID AIR

Xihua He
Center for Nuclear Waste Regulatory Analyses
Southwest Research Institute®
6220 Culebra Road
San Antonio, Texas 78238
E-mail: xhe@swri.org
Telephone: (210) 522-5194

Tae Ahn
U.S. Nuclear Regulatory Commission
Office of Nuclear Material Safety and Safeguard
11545 Rockville Pike
Mail Stop (EBB-2-B02)
Washington, DC

Timothy Sippel
U.S. Nuclear Regulatory Commission
Office of Nuclear Material Safety and Safeguard
11545 Rockville Pike
Mail Stop (EBB-2-B02)
Washington, DC

ABSTRACT

Borated stainless steel alloys are candidate neutron absorber materials for criticality control in disposal containers or dry storage canisters. Type 304 borated stainless steels are similar to conventional Type 304 stainless steels except that they contain a boron addition, which imparts a much higher thermal neutron absorption cross section than other austenitic stainless steels. This work investigated the corrosion behavior of borated stainless steel in water and humid air. In this study, Type 304B4 and 304B5 borated stainless steels were exposed to the liquid and vapor phases of simulated groundwater at 60, 75, and 90 °C [140, 167, and 194 °F] for about 3 months. The vapor phase was open to air representing the humid air condition. The posttest specimens were analyzed to determine general corrosion rates and occurrence of localized corrosion. It was found that some specimens exposed to humid air at 75 and 90 °C [167 and 194 °F] suffered pitting corrosion, but pitting corrosion was not observed at 60 °C [140 °F] or from the liquid exposure at 75 and 90 °C [167 and 194 °F]. The pits were circular, and the surface near the pitted area was stained. The maximum pit depth was about 70 µm [2.8 mil]. All the specimens exposed to the liquid phase showed weight gain before acid cleaning of the surface due to scale formation. Most of the specimens exposed to humid air showed weight loss. At all three temperatures, the general corrosion rates of Type 304B4 were less than 80 nm/yr [0.0032 mil/yr] and those of Type 304B5 were less than 600 nm/yr [0.024 mil/yr]. No clear trend was observed regarding the influence of temperature on general corrosion rates of each material. The general corrosion rates of Type 304B5 were higher than those of Type 304B4.

Keywords: Borated stainless steel, boron, corrosion, liquid, vapor

INTRODUCTION

For criticality control of spent nuclear fuel in disposal and dry storage, candidate neutron absorber materials are borated stainless steel alloys, borated aluminum alloys, and boron carbide-aluminum alloy composites. Boron used in these neutron absorber materials may be natural or enriched in the nuclide B-10. The boron is usually incorporated either as an intermetallic phase (e.g., AlB_2, TiB_2, CrB_2) in an aluminum alloy or stainless steel, or as a stable chemical compound particulate, such as boron carbide (B_4C), typically in an aluminum metal-matrix composite or cermet.[1]

Type 304 borated stainless steels are similar in composition to conventional Type 304 stainless steels except that they contain boron, which imparts a much higher thermal neutron absorption cross section than other austenitic stainless steels. The solubility of boron in stainless steel is low, and the production of alloys with more than 2.25 wt% boron content is difficult. ASTM A887–89[2] defines eight types (304B, 304B1–304B7) of borated stainless steels with boron concentrations from 0.2 to 2.25 wt%. Increasing boron content increases the thermal neutron absorption capabilities, hardness, tensile strength, and yield strength, but decreases tensile ductility, impact toughness, and corrosion resistance. For each type of borated stainless steel with the same chemical composition, ASTM A887–89 specifies two grades (A and B) defined by the uniformity of boron dispersion within the melt. According to ASTM A887–89, Grade A corresponds to the near-optimal boron dispersion, while Grade B corresponds to a less-than-optimal dispersion of the boron. The difference in uniformity of boron dispersion leads to a difference in material ductility and toughness. ASTM A887–89 specifies that Grade A has increased impact and tensile testing requirements compared to those for Grade B. Historically, the only way to meet the Grade A requirements was to produce material via a powder metallurgy technique. Conventional cast-and-wrought metallurgical practice is able to reach Grade B properties; however, ASTM International does not preclude the use of powder metallurgy techniques in the supply of Grade B materials. EPRI[3] lists two available products conforming to ASTM A887–89 specifications: NeutroSorb (Carpenter Powder Products, USA) and Neutronit (Bohler Bleche GmbH, Austria).

Borated stainless steel alloys solidify as primary austenite with a terminal eutectic constituent, which has the form $(Fe, Cr)_2B$, with the exact composition dependent on the initial boron level.[4] The austenite matrix is a ductile phase, and the dispersed secondary phase is a comparatively brittle compound. With the same chemical composition, the metallurgical structure differs depending on the fabrication techniques. For the products produced by the powder metallurgy technique, the secondary phase is finer and more uniformly distributed compared to those provided by the cast-and-wrought process. The Grade B material produced by the powder metallurgy technique has a consistent microstructure along the cross section compared to that produced by the cast-and-wrought technique. The difference in microstructure usually leads to a difference in mechanical properties and corrosion resistance. Powder metallurgy material tends to have higher corrosion resistance and easily meets ASTM A887–89 specification requirements.

These borated stainless steel alloys have been used in the nuclear industry for spent fuel storage and transportation racks and cask baskets, control rods, burnable poison, and shielding to control the reactivity of spent nuclear fuel.[5] Use of neutron absorber materials allows storage and shipment of spent fuel at maximum packing density and, therefore, is more cost effective. In the past several years, the Type 304 stainless steel (UNS S30400) racks of nuclear power plant pools have been replaced by borated stainless steel racks to increase their storage capacity, as borated stainless steel has a greater neutron absorption capacity than other

neutron absorber materials. In terms of matrix durability, stainless steel represents the neutron absorber material with the most stable matrix for wet and dry storage service environments.

Review of General Corrosion of Borated Stainless Steels

Several researchers[6-12] have investigated the corrosion performance and the general corrosion rates of unborated Types 304 and 316 series stainless steels and borated stainless steels in J-13 well water environments and in in-package conditions relevant to the potential arid repository for temperatures in the 0–100 °C [32–212 °F] range. In relatively benign environments with low chloride concentration and near-neutral pH, borated stainless steels performed similarly to conventional unborated stainless steels.[13–14] However, in a more corrosive environment, Cole[15] has shown that increasing boron content increases the corrosion rate of borated stainless steel and increasing temperature enhances the difference between borated and unborated stainless steel.

The corrosion rate for Types 304 or 316 stainless steels in the typical J-13 well water environment ranges between 0.02–0.57 µm/yr [0.0008–0.022 mil/yr] in test durations from less than 100 hours to more than 11,000 hours. In the vapor phase, Beavers and Durr[8] observed higher corrosion rates than those in liquid. One comparison study[13] of borated versus unborated 304L stainless steel in a low pH environment showed that the borated material (with 1.23 wt% B) had a corrosion rate that was four times that of the unborated material. EPRI[14] indicated that borated stainless steels with boron contents between 1–2 percent showed lower resistance to general, pitting, crevice, and intergranular corrosion in harsh (boiling acidic and/or high Cl^-) environments as boron content increases. However, a 6-month test in more benign spent fuel pool conditions of 68 °C [154 °F] and pH of 5.3 (2,000 ppm boric acid) showed no difference in corrosion resistance for stainless steel with boron concentrations of 1 to 1.75 percent.[14] Cole[15] shows that in hydrofluoric acid and hydrochloric-acid-containing solution, stainless steel alloyed with 1.5 percent boron degraded faster than stainless steel containing only 0.3 percent boron.

Lister, et al.[11-12] evaluated the long-term corrosion resistance performance of Types 304B4 and 304B5 borated stainless steels under exposure to an expected arid repository conditions after a waste package breach. The results show that corrosion rates were less than 50 µm/yr [0.002 mil/yr] for the test period of less than 600 hours.

Review of Localized Corrosion of Borated Stainless Steels

In addition to the difference in general corrosion, the localized corrosion behavior of borated stainless steels is also different from unborated stainless steels mainly due to the presence of the secondary phase dispersed in the austenitic matrix as schematically shown in Figure 1. Information in the literature indicates that attack of the regions surrounding the particles has been attributed to a depletion of chromium at these regions. Moreno, et al.[16] studied the pitting corrosion behavior of borated stainless steel in chloride and sulfide media. The authors observed that the chromium boride particles [$(Cr_2Fe)_{7.66}(B,C)_6$] in an austenitic matrix belong to a face-centered cubic system. The authors observed a greater number of pits in the chloride medium, and the pitting was more extended at a subsurface level but was not obvious at the surface. In the sulfide medium, the pits were not as deep, but they extended further along the surface. The pitting potentials in the sulfide medium were higher than those obtained in the chloride medium. The pits were reported to nucleate at secondary phase particles.

Grade B materials produced by the cast-and-wrought metallurgical process are known to have lower corrosion resistance due to the larger irregular particle distribution.[17] Long-term immersion testing of Grade B materials has been performed to evaluate the corrosion performance versus conventional austenitic materials in simulated concentrated groundwater solutions at 90 °C [194 °F].[18] Overall, these tests showed extensive localized corrosion for the Grade B materials in comparison to the conventional austenitic materials.

Lister, et al.[10-12] also studied the localized corrosion resistance of borated stainless steels exposed to arid repository conditions. While the corrosion potential of these materials stabilized at 40 mV versus a saturated calomel electrode, no signs of negative variation from stable potential due to pitting corrosion were observed.[11] Tests showed that Grade A material had better localized corrosion performance than Grade B. In addition, the localized corrosion resistance reduced with an increasing amount of boron in the Grade A alloys. The authors observed that the austenite matrix was etched surrounding the boride particles and the secondary phase $(Fe, Cr)_2B$ was stable. Solution analysis using the inductively coupled plasma-mass spectrometry method showed that the boron concentration was under the detection limit in solution, so the authors indicated that boron remained with the secondary phase particles.[10,11]

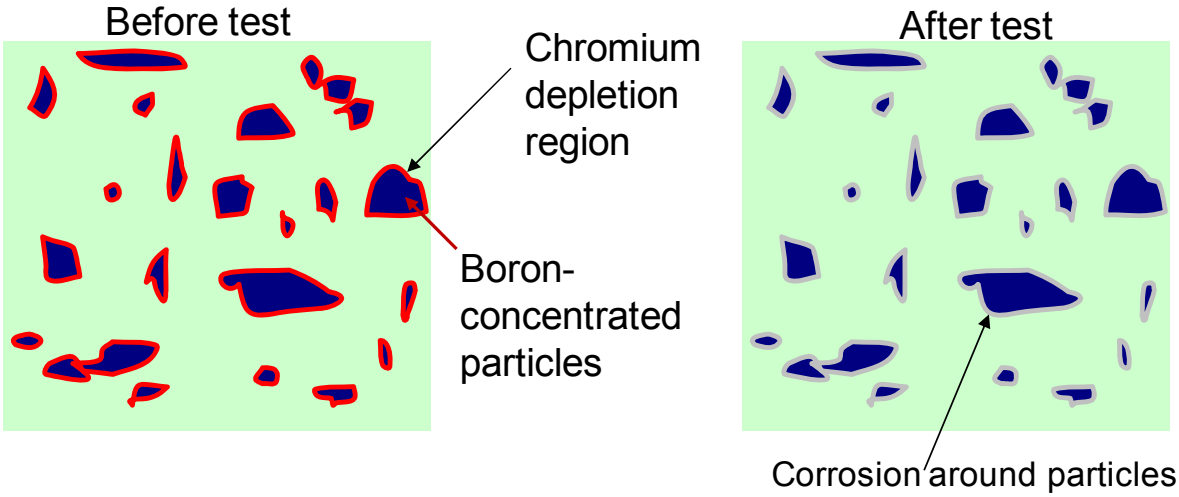

Figure 1: Schematics showing the chromium boride particles dispersed in an austenitic matrix and preferential corrosion around the particles

The general corrosion and localized corrosion resistance of borated stainless steels is important in evaluating materials performance in criticality control. During geological waste disposal and extended storage, corrosion of borated stainless steel could occur in a humid air environment. As shown in the previous literature review, the corrosion data under a humid air condition is scarce. The objective of this work is to investigate the corrosion behavior of borated stainless steels in humid air conditions and compare it to that obtained from water. The test results can be used to understand the corrosion performance of this type of material in criticality control applications.

EXPERIMENTAL METHODS

Test Preparation and Test Process

Two alloys, Types 304B4 Grade B and 304B5 Grade A, were used in the tests in accordance with ASTM A887–89[2]. These alloys were purchased from Carpenter Powder Products (the Micro-Melt NeutroSorb products in Table 1) in sheet stock (Grade B of Type 304B4 and Grade A of Type 304B5 were purchased because these are the only available grades from the supplier). The thickness of the sheet was about 3.8 mm [0.15 in]. According to the supplier, these alloys were fabricated from the powder metallurgy technique. Table 1 shows the heat numbers and the chemical composition of these two alloys (the chemical composition from independent analysis is consistent with that provided by the supplier).

Figure 2 shows the microstructure of these two materials. The sample was etched with the Kalling's reagent {40 mL [1.4 fl oz] H_2O, 2 g [0.004 lb] $CuCl_2$, 40 mL [1.4 fl oz] HCl, 40 mL [1.4 fl oz] ethanol} at ambient temperature for 10–20 seconds to bring out the dispersed boride structure in an austenite matrix. In both materials, the boride particles were circular and in the micron range. There were more particles in Type 304B5 than in Type 304B4, probably due to the higher boron concentration in Type 304B5. The particles were finely dispersed in the matrix, consistent with the powder metallurgy material. It seems that the bulk of the matrix was not etched by the Kalling's reagent, and no grain boundaries were observed.

Specimens with a length of 10.2 cm [4 in] and a width of 3.18 cm [1.25 in] were machined from the sheet stock of the supplied material. The total surface area of each specimen was about 75 cm^2 [12 in^2] considering that the thickness of the specimen was 3.8 mm [0.15 in]. The specimens were polished with sandpaper up to 600 grit, ultrasonically cleaned in deionized water, and dried in acetone. Figure 3 shows examples of the finished specimens before the test.

Three glass cells with polytetrafluoroethylene lids were used in the test. The solution used was simulated groundwater as in He, et al.[19] Each simulated water was prepared from two stock solutions, A and B, listed in Table 2a. Before use, equal amounts of stock solutions were mixed and diluted fortyfold to prepare the simulated water. The calculated composition and measured pH is shown in Table 2b. A solution volume of 1.2 L [0.32 gal] was added to each cell.

Each cell contained six specimens of each material: three immersed in liquid and the other three exposed in vapor. This resulted in 18 specimens of each material for all the tests. For specimen identification, the specimens were engraved consecutively from B4-1 to B4-18 for Type 304B4 stainless steel, and B5-1 to B5-18 for Type 304B5 stainless steel. A house-made, six-tier polytetrafluoroethylene rack was used in each cell to hold the specimen, with two specimens on each tier, one from each material. Each tier of the polytetrafluoroethylene rack was constructed from a round-hole-perforated polytetrafluoroethylene sheet 1.59 mm [0.0625 in] thick to increase the material contact with liquid or vapor and avoid forming an occluded region under the specimens. The diameter of the round hole was 3.18 mm [0.125 in], and the opening area of the sheet was about 40 percent. Tests were performed at 60, 75, and 90 °C [140, 167, and 194 °F] maintained by thermocouple-based temperature controllers. The heating was supplied by a mantle around the cell. The temperature of the cell was confirmed using a calibrated thermometer before initiating the test.

Table 1: Alloy composition and ASTM specifications (wt%)				
Alloy	Type 304B4 Grade B Heat 172862	Type 304B4 Specification in ASTM A887–89*	Type 304B5 Grade A Heat 182019	Type 304B5 Specification ASTM A887–89*
Cr	19.40	18.00–20.00	18.28	18.00–20.00
Ni	14.11	12.00–15.00	13.61	12.00–15.00
B	1.04	1.00–1.24	1.34	1.25–1.49
C	0.009	0.08	0.032	0.08
N	0.0054	0.10	0.021	0.10
P	0.008	0.045	0.018	0.045
S	0.005	0.030	0.001	0.030
Co	0.02	0.20	0.05	0.20
Si	0.59	0.75	0.73	0.75
Mn	1.65	2.00	1.83	2.00
Mo	0.01	Not available	0.02	Not available
Cu	0.01	Not available	0.04	Not available
Fe	balance	balance	balance	balance

*Maximum, unless range or minimum is indicated
Cr = chromium, Ni = nickel, B = boron, C = carbon, N = nitrogen, P = phosphorous, S = sulfur, Co = cobalt, Si = silicon, Mn = manganese, Mo = molybdenum, Cu = copper, Fe = iron

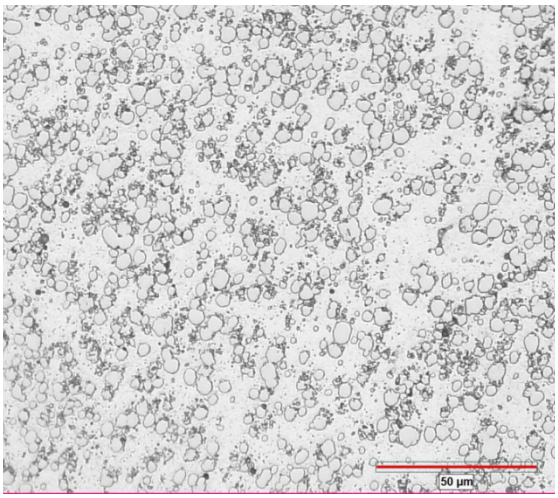

Type 304B4 Grade B

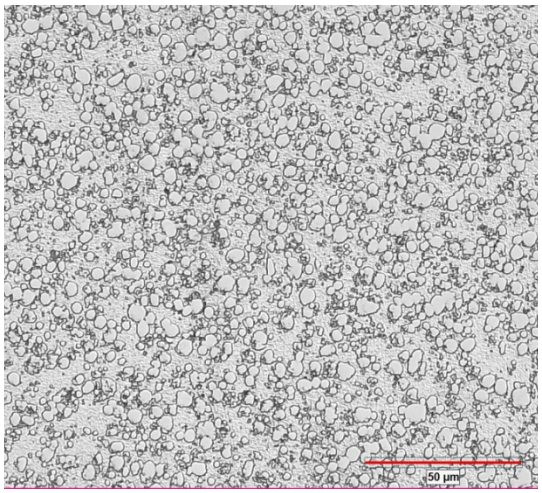

Type 304B5 Grade A

Figure 2: Optical metallurgraphs of Type 304B4 Grade B and Type 304B5 Grade A stainless steels etched with Kalling's reagent

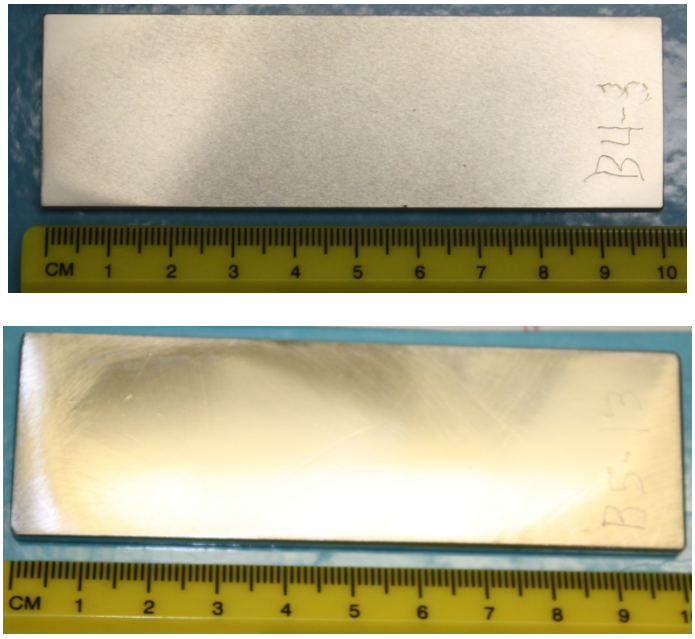

Figure 3: Finished borated stainless steel specimen examples before the test

Table 2a: Stock solutions A and B for simulated groundwater preparation			
Stock Solution A		Stock Solution B	
Chemical Reagents	Concentration (g/L*)	Chemical Reagents	Concentration (g/L*)
$CaSO_4 \bullet 2H_2O$	1.374	$NaHCO_3$	6.720
$Ca(NO_3)_2 \bullet 4H_2O$	0.942		
KCl	0.116	NaF	0.169
$MgCl_2$	0.267		
*1 g/L = 8.35×10^{-3} lb/gal			

Table 2b: Chemical composition of simulated groundwater									
$[Ca^{2+}]$ mg/L*	$[K^{+}]$ mg/L	$[Mg^{2+}]$ mg/L	$[Na^{+}]$ mg/L	$[SO_4^{2-}]$ mg/L	$[NO_3^{-}]$ mg/L	$[Cl^{-}]$ mg/L	$[F^{-}]$ mg/L	$[HCO_3^{-}]$ mg/L	Measured pH
12.0	3.83	1.70	46.0	19.2	12.4	6.33	1.92	122	8.05
*1 mg/L = 8.35×10^{-6} lb/gal									

The cell was fitted with a condenser to prevent solution loss while maintaining atmospheric pressure during the test. The condenser was circulated with room temperature water. An image of the test cell with specimens, solution, condenser, and thermocouple is shown in Figure 4.

During testing, the cell temperature and solution level were monitored. Some solution was lost due to evaporation, especially when the cell reached 90 °C [194 °F]. The lost solution was compensated with fresh solution weekly to maintain the original volume. Additionally, some solution condensed on the specimens exposed in vapor. The cell was tilted slightly to facilitate flow of condensation off the specimen, and the cell was shaken weekly to remove the condensation.

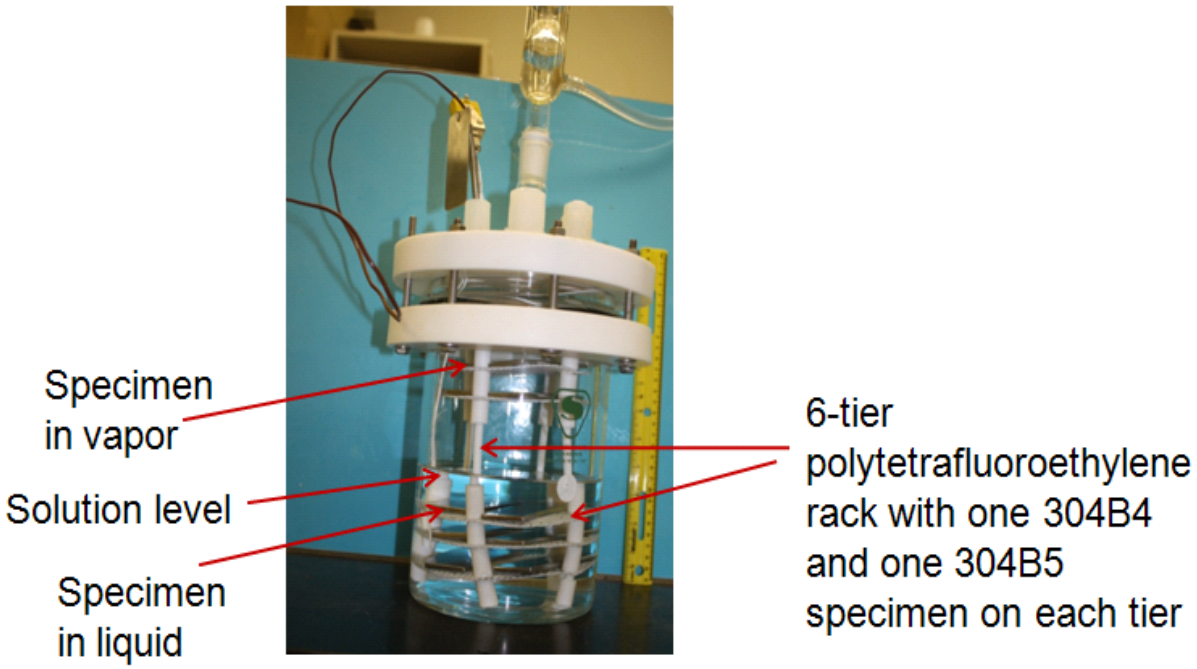

Figure 4: Image of glass test cell used in the test with simulated groundwater, Types 304B4 and 304B5 specimens, condenser, and thermocouple

Posttest Analysis

The test duration was 106 days, shorter than what ASTM G31[20] suggested {for an average corrosion rate of 50 nm/yr [0.0019 mpy], the test duration in hours suggested in ASTM G31 (Section 8.11.4) is 1×10^6 hours}. After the test, the specimens were cleaned ultrasonically with deionized water, dried with acetone, and weighed immediately. The water-cleaned and dried specimens were photographed. The specimens were cleaned with solution for 20 minutes at 60 °C [140 °F] along with a control specimen to obtain weight loss in accordance with ASTM G1-03.[21] For some specimens with localized corrosion, after the rust was removed by the 10 percent HNO_3 cleaning solution, the corroded area was observed under optical microscope and some areas were scanned with a three-dimensional (3-D) laser profilometer to map the corrosion damage. Depending on the adherence of the scales formed on the surface, some specimens were cleaned multiple times until a constant weight or minor weight gain was observed.

The weight loss from specimens without pitting corrosion was calculated for general corrosion rates using Equation (1).[21]

$$CR = (8.76 \times 10^7)\times(\Delta m)/(\rho t A) \qquad \text{Equation (1)}$$

where

CR = Corrosion rate, nm/yr
Δm = Weight loss, mg
ρ = Material density, g/cm^3
t = Test duration, hours

A = Surface area, cm^2

The density is 7.81 g/cm^3 [0.282 lb/in^3] for Type 304B4 stainless steel and 7.79 g/cm^3 [0.281 lb/in^3] for Type 304B5 stainless steel.[22]

RESULTS AND DISCUSSION

The tests were terminated after about 3 months. For all the tests, the solution was clear and no visible solids were observed after the tests. For the test at 90 °C [194 °F], the solution was slightly yellowish. The pH of the solution was 9.07, 9.34, and 9.70 for the tests at 60, 75, and 90 °C [140, 167, and 194 °F], respectively, which was higher than the original pH shown in Table 2b. Figures 5 to 12 show a pictorial record of the top side and back side of all the posttest 304B4 and 304B5 specimens. The weight changes of these specimens right after the test and after 10 percent HNO_3 cleaning are summarized in Table 3. The general corrosion rates were plotted in Figure 13.

At 60 °C [140 °F] for both Types 304B4 and 304B5 materials (Figures 5 and 6, Table 3), the following observations were made.

- In liquid and vapor, there was no localized corrosion feature visible by naked eye or microscope except for some deposits and water staining on some specimens (e.g., specimens B4-2, B4-3). The polishing marks were still visible.

- Right after the test and before cleaning with 10 percent HNO_3, all the specimens exposed in liquid showed weight gain. Specimen B4-4 exposed to vapor showed weight gain, and Specimen B4-6 showed no weight change. Other specimens excluding B4-4 and B4-6 exposed to vapor showed weight loss.

- After the first cleaning with 10 percent HNO_3 at 60 °C [140 °F] for 20 minutes, all the specimens showed weight loss. Subsequent cleaning showed minor weight change, so, consistent with ASTM G1–03[21], the weight loss from the first 10 percent HNO_3 cleaning was used to calculate the corrosion rate.

- All the corrosion rates of Type 304B4 were less than 60 nm/yr [0.0024 mil/yr]. All the corrosion rates of Type 304B5 were less than 200 nm/yr [0.00787 mil/yr]. The corrosion rates of Type 304B5 material were higher than those of Type 304B4 material.

- For Type 304B4, the average corrosion rates from the vapor phase were higher than those from the liquid phase, but they were similar for Type 304B5.

At 75 °C [167 °F] for Type 304B4 (Figure 7, Table 3), the following observations were made.

- In both liquid and vapor phases, the surface of all materials was covered with a thin layer of scale which masked the polishing lines. All the specimens exposed in liquid showed weight gain. Except for weight loss from specimen B4-10, the other two specimens exposed in vapor showed weight gain. Within the scatter of data, weight loss is determined if the oxide dissolution is appreciable.

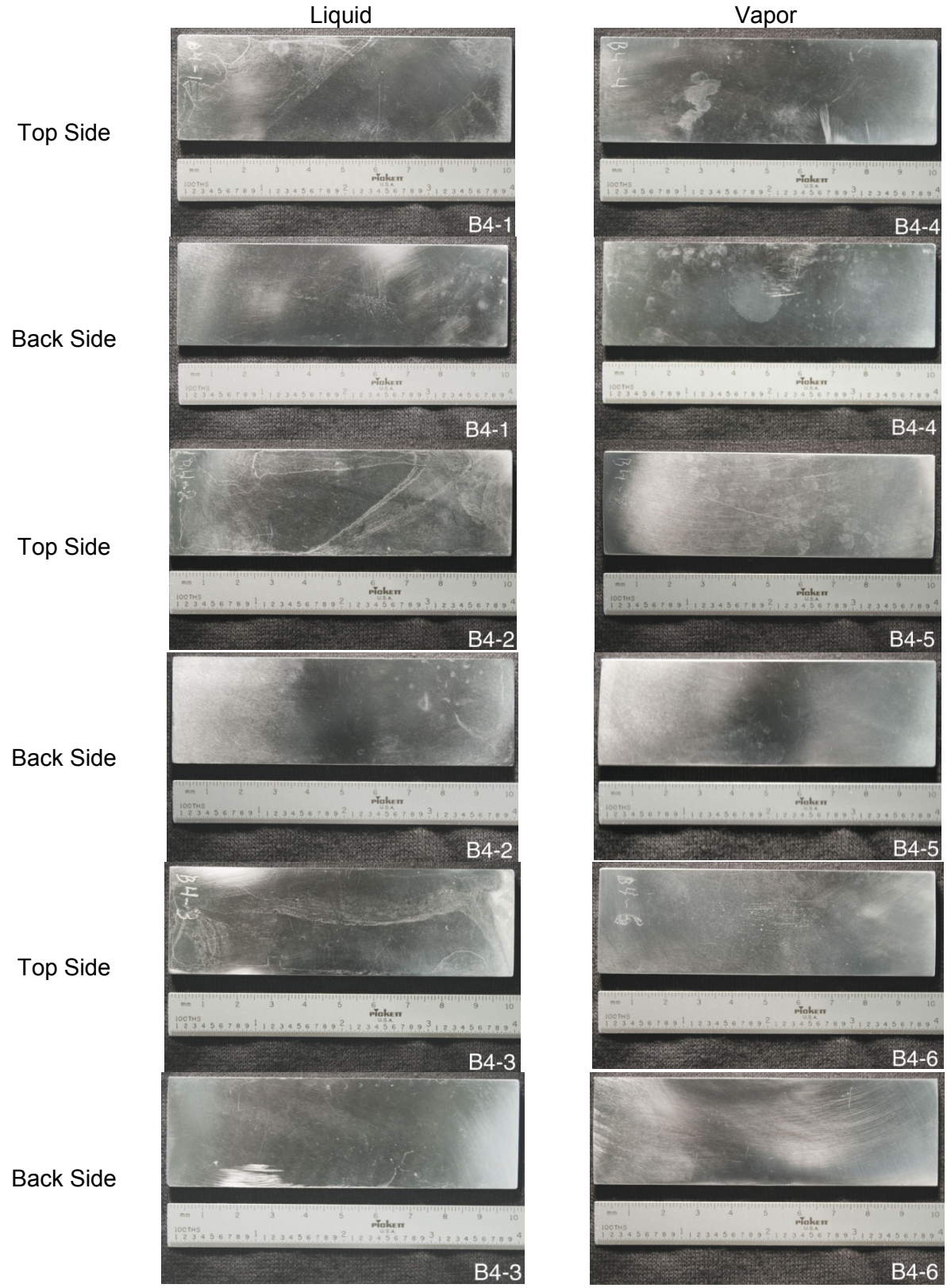

Figure 5: Photos of Type 304B4 borated stainless steel specimens after test in simulated groundwater at 60 °C [140 °F]

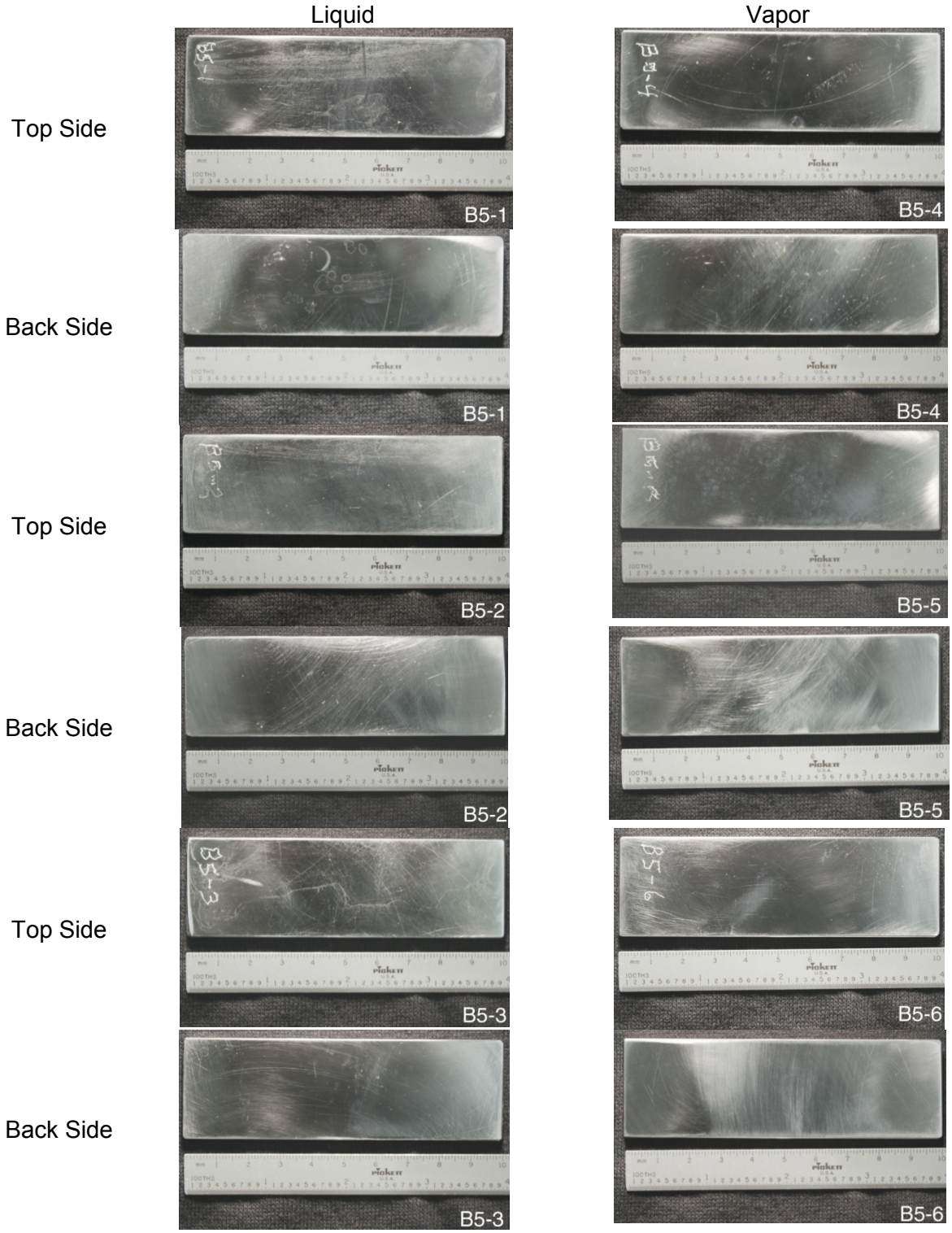

Figure 6: Photos of Type 304B5 borated stainless steel specimens after test in simulated groundwater at 60 °C [140 °F]

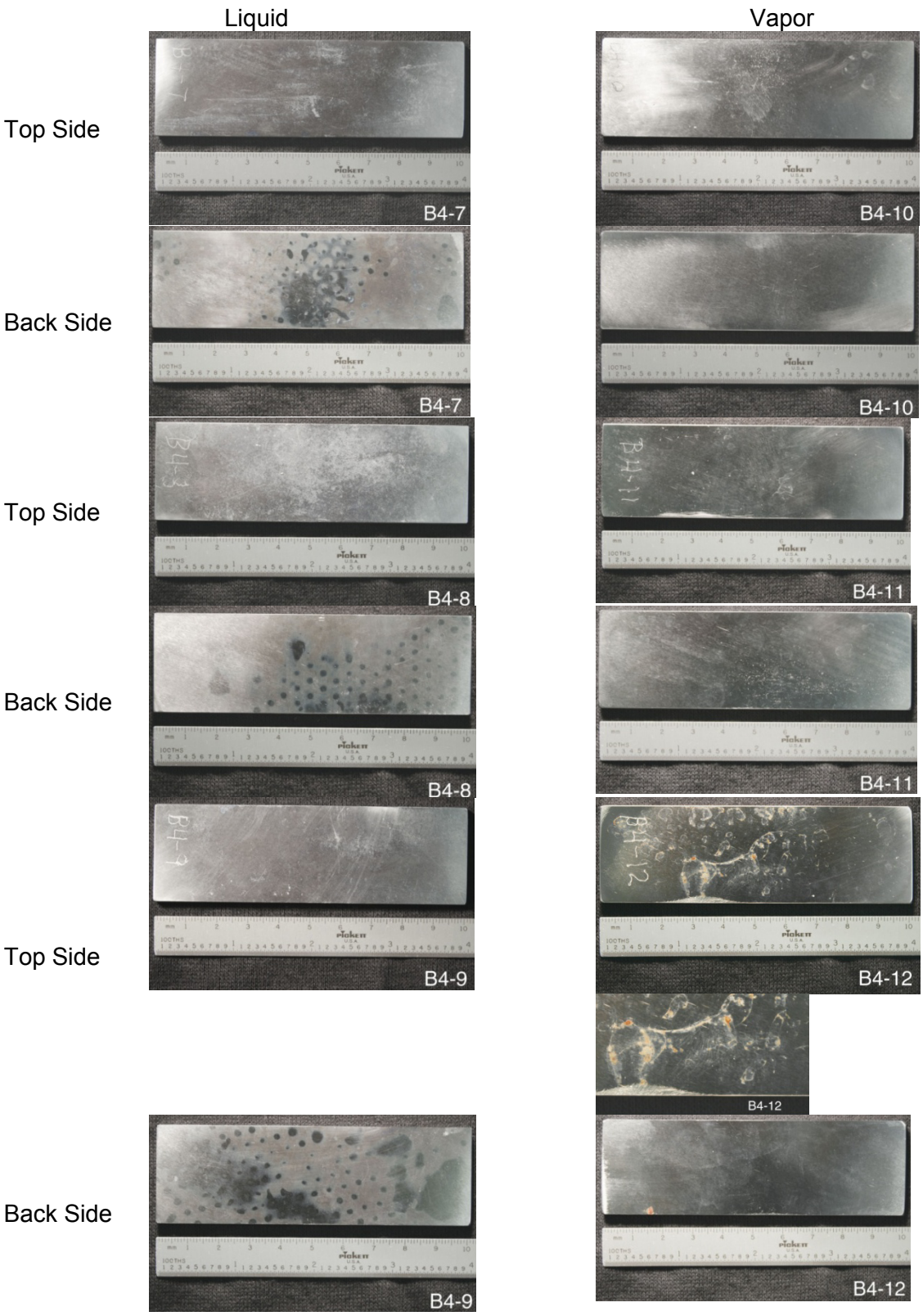

Figure 7: Photos of Type 304B4 borated stainless steel specimens after test in simulated groundwater at 75 °C [167 °F]

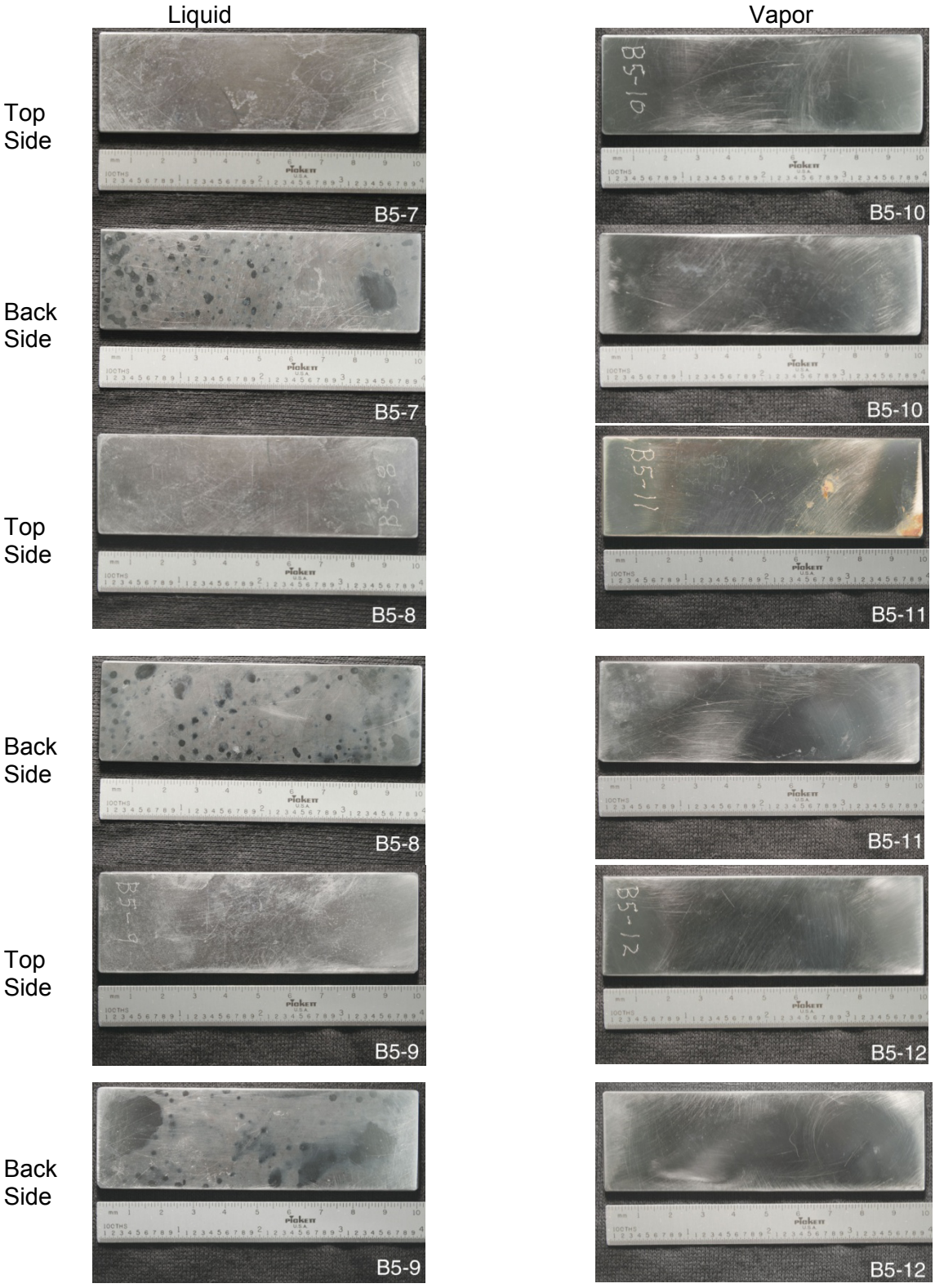

Figure 8: Photos of Type 304B5 borated stainless steel specimens after test in simulated groundwater at 75 °C [167 °F]

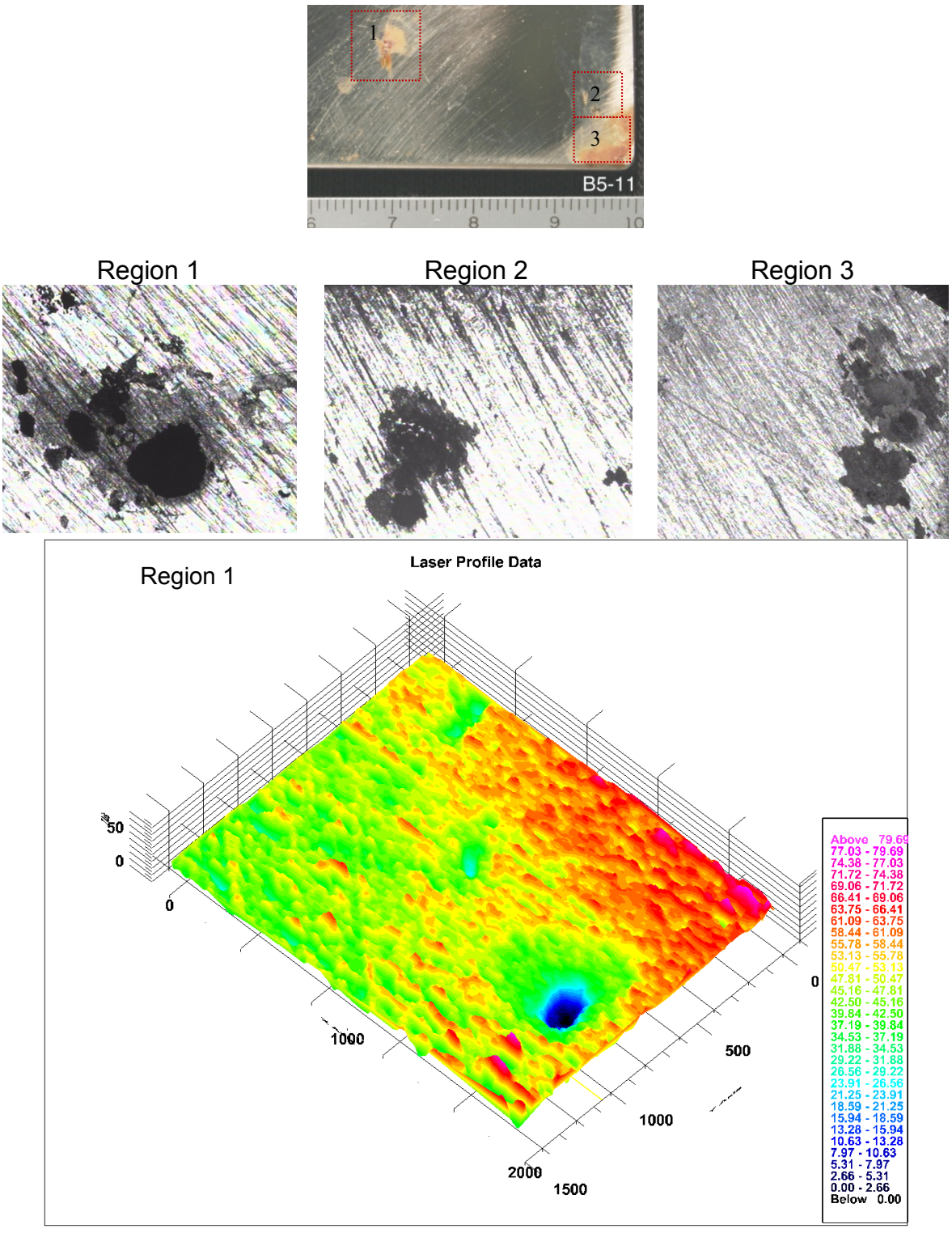

Figure 9: Optical photos and 3-D laser profilometer scans of areas with pitting corrosion for specimen 304B5-11. (The scale for the optical photo in the left column is not available due to limitation of the equipment. The numbers in the laser profile data at right side are depth in units of μm.)

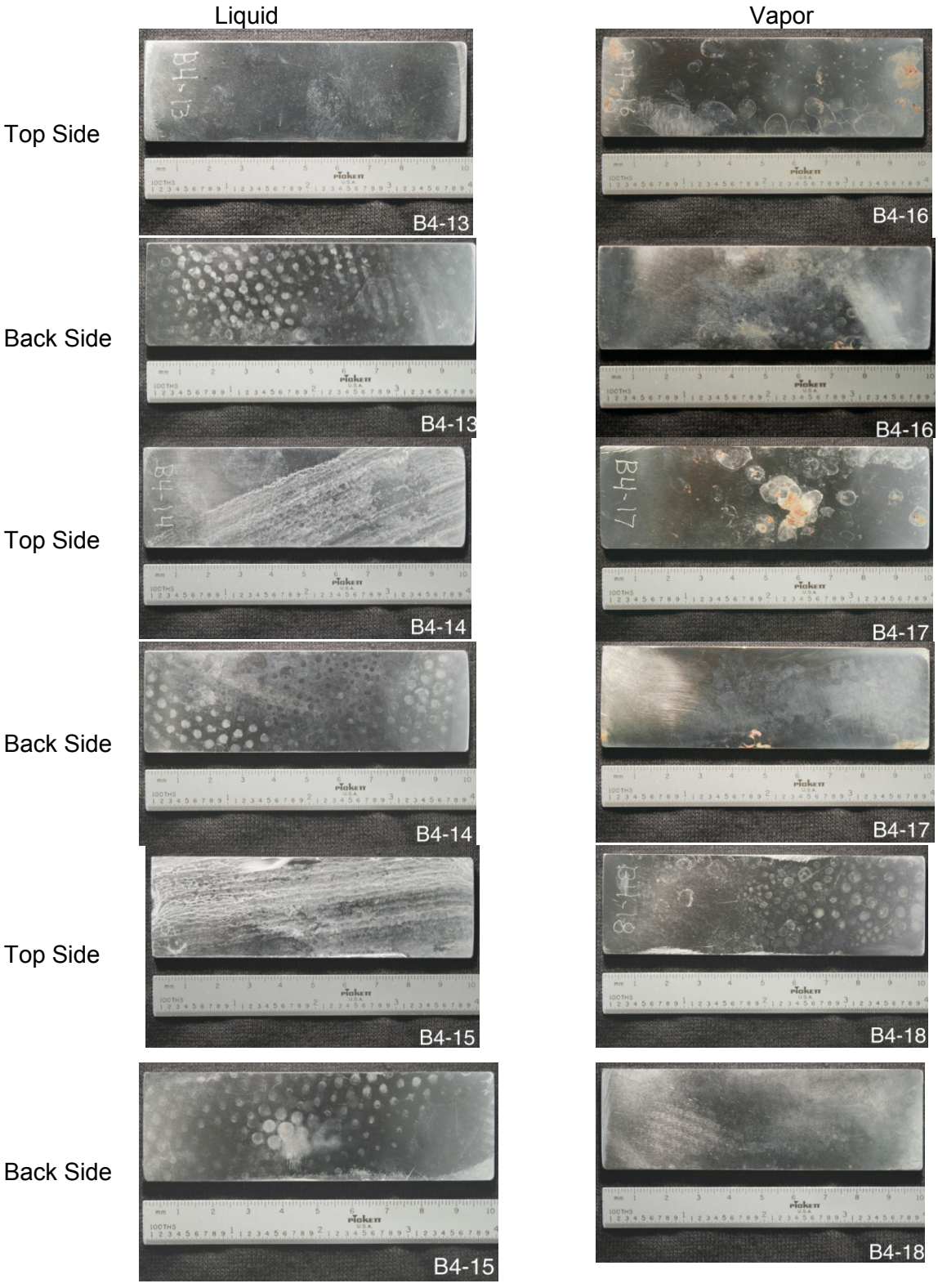

Figure 10: Photos of 304B4 borated stainless steel specimens after test in simulated groundwater at 90 °C [194 °F]

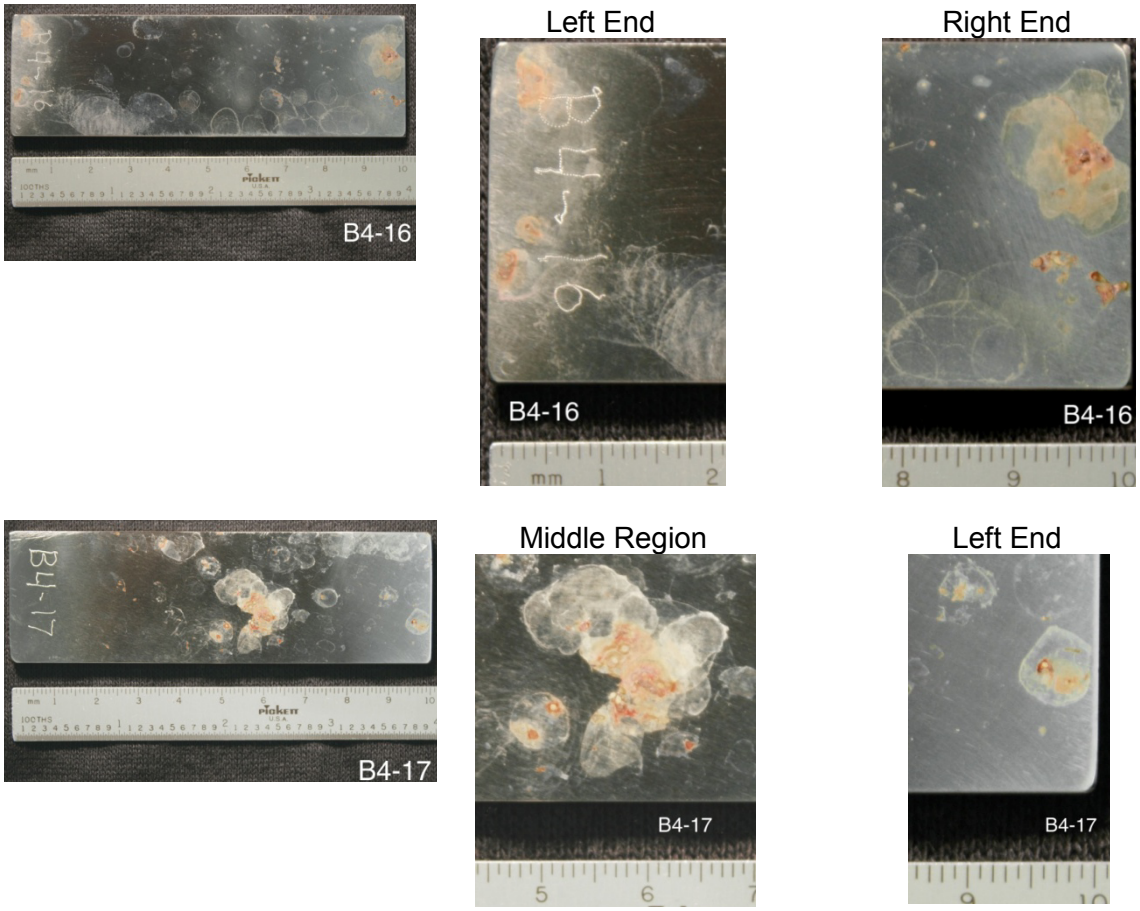

Figure 11: Optical photos of areas with pitting corrosion for specimens Type 304B4-16 and Type 304B4-17

- The scales on the surface adhered tightly. It took multiple attempts to clean the surface.
- For all specimens in liquid, some areas of the back side had copied the pattern of the perforated polytetrafluoroethylene sheet used to hold the specimen.
- Specimen B4-12 exposed to vapor suffered pitting corrosion, mostly at the top side. One photo with higher magnification is shown in Figure 7. The surface of the sample near the pitted area was stained. These stains were likely caused by corrosion products leaching from the pits and precipitating into high-pH regions. After first cleaning with 10 percent HNO_3 solution, the rust on the surface was removed and the specimen was examined under the microscope. The pits were very shallow with nonmeasurable depth.
- All the corrosion rates of Type 304B4 were less than 40 nm/yr [0.0016 mil/yr].
- The average corrosion rates from the vapor phase were higher than those from the liquid phase.

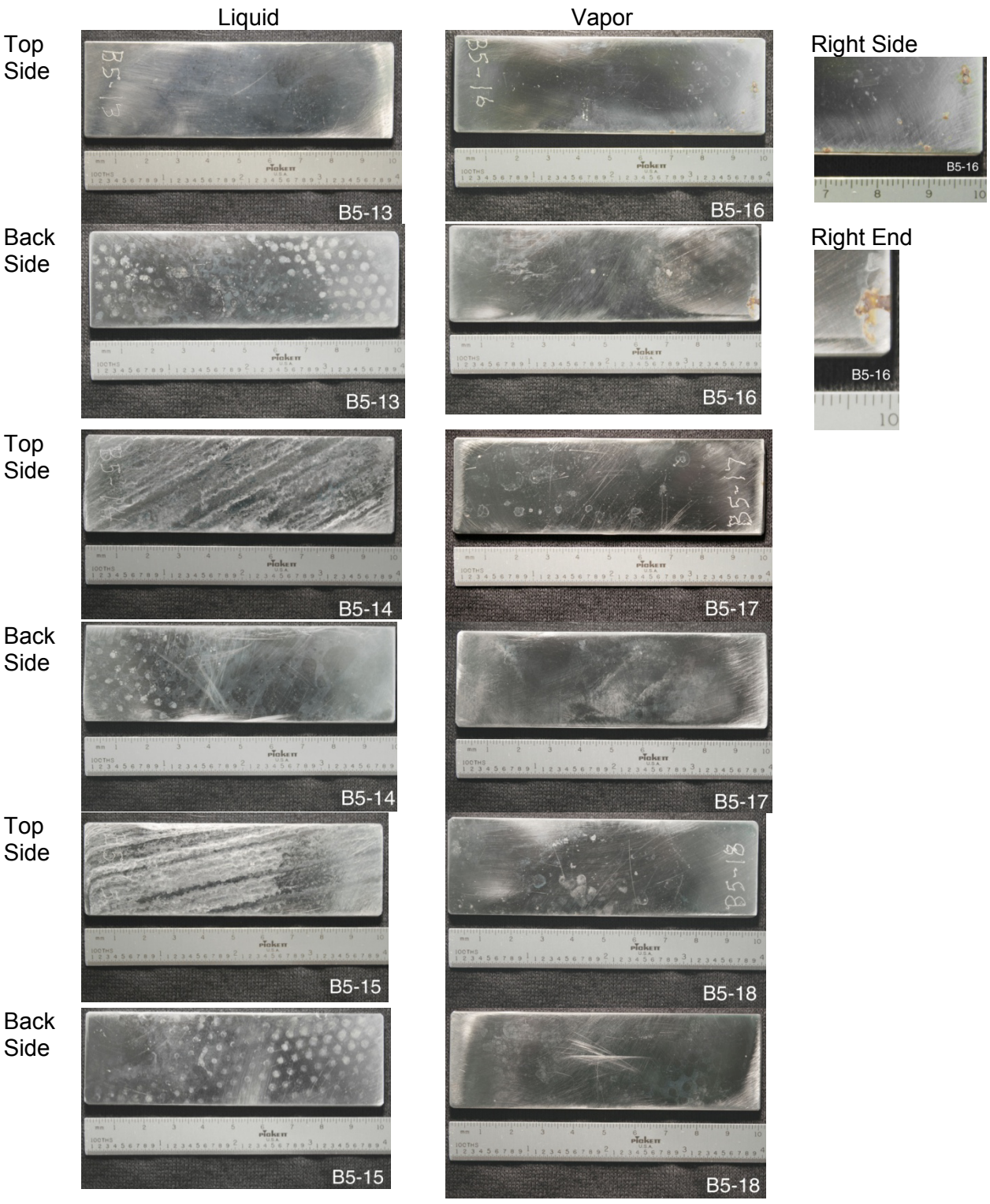

Figure 12: Photos of 304B5 borated stainless steel specimens after test in simulated groundwater at 90 °C [194 °F]

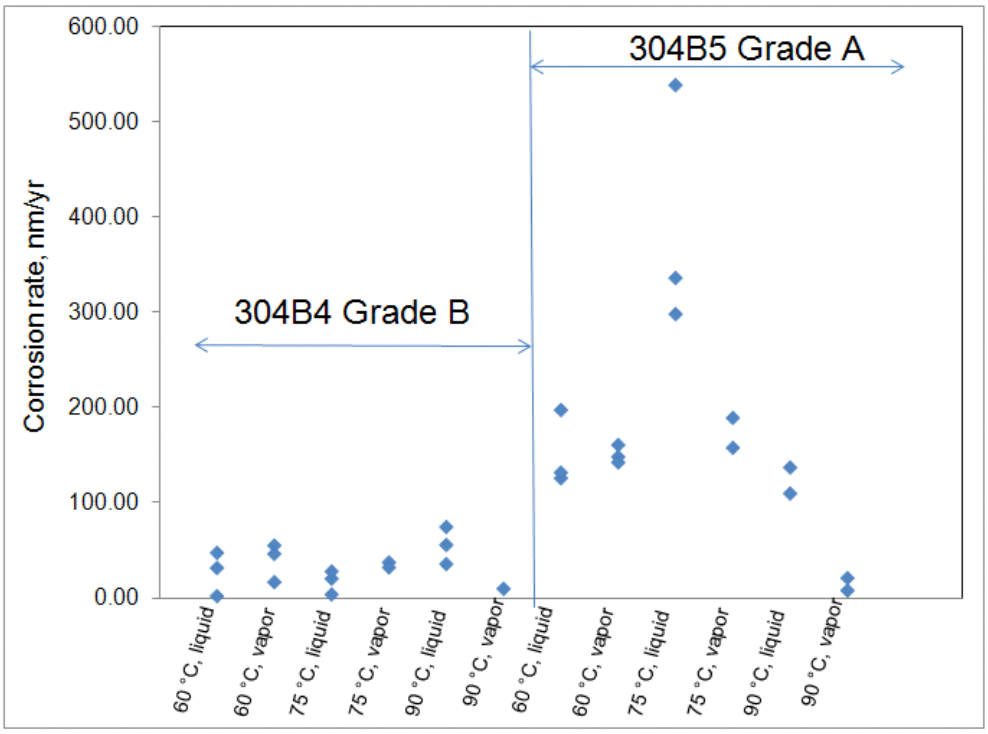

Figure 13: General corrosion rates of 304B4 and 304B5 specimens exposed in liquid or vapor at 60, 75, and 90 °C [140, 167, and 194 °F]

At 75 °C [167 °F] for Type 304B5 (Figures 8 and 9, Table 3), the following observations were made.

- In both liquid and vapor phases, the surface of all materials was covered with a thin layer of scales masking the polishing lines, which is similar to the results for Type 304B4.
- All the specimens exposed in liquid showed weight gain, and all the specimens exposed in vapor showed weight loss, indicating the occurrence of corrosion.
- The scales on the surface adhered tightly. It took multiple attempts to clean the surface.
- For all specimens in liquid, some areas of the back side had copied the pattern of the perforated polytetrafluoroethylene sheet used to hold the specimen.
- The top side of specimen B5-11 exposed in vapor suffered pitting corrosion. After first cleaning with 10 percent HNO_3 solution, the specimen was examined under the microscope. The deepest penetration was about 74 µm [2.9 mil]. Figure 9 shows optical photos of several pitted areas and the 3-D laser profilometer mapping images of several large pits. Most of the pits were circular, and the diameter of the large pits at the surface was about 500 µm [19.7 mil], which is larger than the secondary boride particles. The pit got smaller while penetrating deeper into the material. The laser profilometer showed that

Table 3: Weight change and corrosion rates of all 304B4 and 304B5 specimens

Tests	Sample ID	Weight change before cleaning with 10 percent HNO_3	Weight change after with cleaning 10 percent HNO_3	Corrosion rate, nm/yr	Sample ID	Weight change before cleaning with 10 percent HNO3	Weight change after with cleaning 10 percent HNO_3	Corrosion rate, nm/yr
60 °C [140 °F] Liquid	B4-1	+1.17	−0.04	2.36	B5-1	+0.70	−2.13	126
	B4-2	+1.45	−0.54	31.9	B5-2	+1.27	−2.23	132
	B4-3	+2.51	−0.81	47.8	B5-3	+0.93	−3.34	198
	Average Corrosion Rate ± Standard Deviation, nm/yr			27.3 ± 23.0				152 ± 40
60 °C [140 °F] Vapor	B4-4	+0.45	−0.29	17.1	B5-4	−0.47	−2.51	148
	B4-5	−0.31	−0.94	55.5	B5-5	−0.58	−2.41	142
	B4-6	0	−0.79	46.6	B5-6	−0.56	−2.72	161
	Average Corrosion Rate ± Standard Deviation, nm/yr			39.8 ± 20.1				150 ± 10
75 °C [167 °F] Liquid	B4-7	+2.61	−0.35	20.7	B5-7	+4.41	−9.10	538
	B4-8	+3.03	−0.07	4.13	B5-8	+3.17	−5.68	336
	B4-9	+2.22	−0.48	28.3	B5-9	+5.81	−5.04	298
	Average Corrosion Rate ± Standard Deviation, nm/yr			17.6 ± 12.4				390 ± 129
75 °C [167 °F] Vapor	B4-10	−0.07	−0.64	37.8	B5-10	−0.36	−2.67	158
	B4-11	+0.29	−0.55	32.5	B5-11	−0.29	−1.44	Pitting*
	B4-12	+0.52	−0.05	Pitting*	B5-12	−0.30	−3.20	189
	Average Corrosion Rate ± Standard Deviation, nm/yr			35.2 ± 3.8				174 ± 22
90 °C [194 °F] Liquid	B4-13	+0.83	−0.61	36.0	B5-13	+0.59	−2.32	137
	B4-14	+1.22	−1.27	75.0	B5-14	+4.32	−1.86	110
	B4-15	+9.22	−0.95	56.1	B5-15†	+7.84	−0.56	N/A†
	Average Corrosion Rate ± Standard Deviation, nm/yr			55.7 ± 19.5				124 ± 19
90 °C [194 °F] Vapor	B4-16	+0.27	−0.22	Pitting*	B5-16	−0.15	−0.45	Pitting*
	B4-17	+0.37	−0.64	Pitting*	B5-17	+0.04	−0.14	8.29
	B4-18	−0.02	−0.17	10.0	B5-18	−0.11	−0.36	21.3
	Average Corrosion Rate ± Standard Deviation, nm/yr			10.0				14.7 ± 9.2

*Because there is pitting corrosion, the general corrosion rate was not calculated based on weight loss.
†The specimen was not completely cleaned with 10 percent HNO_3 and 15 percent HCl even after soaking for 2 days in the solution.

the deepest depth was ~70 µm [~2.8 mil], which is consistent with that measured by optical microscope.

- All the corrosion rates of Type 304B5 were less than 600 nm/yr [0.0236 mil/yr], which is higher than those of Type 304B4 under the same test conditions.
- The average corrosion rates from the liquid phase were higher than those from the vapor phase.

At 90 °C [194 °F] for Type 304B4 (Figures 10 and 11, Table 3), the following observations were made.

- The top surface of specimens B4-14 and B4-15 exposed in liquid was covered with tightly adhered white deposits. However, no visible corrosion was observed for all specimens exposed in liquid.
- All the specimens exposed in liquid showed weight gain before cleaning with acid. Only one specimen (B4-18) exposed in vapor showed weight loss. The other two (B4-16 and B4-17) showed weight gain.
- The average corrosion rates from the liquid were higher than that from the vapor.
- Specimens B4-16 and B4-17 exposed in vapor suffered pitting corrosion. The deepest penetration depth was ~60 µm [~2.4 mil] for B4-16 and ~70 µm [~2.8 mil] for B4-17.

At 90 °C [194 °F] for Type 304B5 (Figure 12, Table 3), the following observations were made.

- Similar to what was observed for Type 304B4 under the same condition, the top surface of specimens B5-14 and B5-15 exposed in liquid was covered with tightly adhered white deposits. The deposits on B5-15 could not be removed by cleaning with 10 percent HNO_3 seven times, nor by soaking in 15 percent HCl solution. However, no visible corrosion was observed for all specimens exposed in liquid.
- All the specimens exposed in liquid showed weight gain before cleaning with acid. Only one specimen (B5-17) exposed in vapor showed weight gain. The other two (B5-16 and B5-18) showed weight loss.
- The average corrosion rates from liquid were higher than that from vapor.
- The corrosion rates were higher than those of Type 304B4 under the same test conditions.
- Specimen B5-16 exposed in vapor suffered pitting corrosion. However, the pit was too shallow to measure.

In summary, Table 3 shows that the general corrosion rates of Type 304B4 were less than 80 µm/yr [0.0032 mil/yr] and those of Type 304B5 were less than 600 µm/yr [0.024 mil/yr]. On average, the general corrosion rates of Type 304B5 were higher than those of Type 304B4. For both materials, no clear trend was observed on temperature effects.

Discussion of Corrosion Test Results on Criticality

Corrosion of borated stainless steel could occur in humid environments during disposal or extended storage. The waste package or canister could be breached which would expose a limited surface opening. Due to capillary effects of water going through the small breached area, the borated stainless steel inside the breached waste package or canister could have humid environments at or above ambient temperatures. Criticality is unlikely to happen when the waste package or the canister is intact or if there is only vapor inside the breached waste package or canister. The vapor itself does not have a sufficient amount of moderation for criticality.

The surface opening area can be large when the waste package or the canister surface is damaged severely by general corrosion over a longer period of time. In this case, the amount of corroded borated stainless steel needs to be estimated for the criticality assessment. The currently measured general corrosion rates may be used to estimate the amount of corroded borated stainless steel. If pitting propagates continuously, the amount of corroded borated stainless needs to be estimated. There could be a limited surface area opening by pitting (e.g., 20 percent).[23] Also, only a fraction of tested coupons in this report showed pitting (e.g., 20 percent). Finally, the criticality assessment may also consider that boron-concentrated particles will remain in the corrosion products of the steel component. Because the duration of the extended storage is shorter than the disposal duration, we expect that there will be less corroded borated stainless steel in the extended storage case.

SUMMARY

In this study, Types 304B4 and 304B5 borated stainless steels were exposed in simulated groundwater in liquid and vapor phases at 60, 75, and 90 °C [140, 167, and 194 °F] for about 3 months. The posttest specimens were analyzed to determine general corrosion rates and occurrence of localized corrosion. The following determinations were made.

- Some specimens of Types 304B4 and 304B5 exposed in vapor at 75 and 90 °C [167 and 194 °F] suffered pitting corrosion, but pitting corrosion was not observed at 60 °C [140 °F] or from the liquid exposure at 75 and 90 °C [167 and 194 °F]. The pits were circular, and the surface near the pitted area was stained. The maximum pit depth was about 70 μm [2.8 mil] at both 75 and 90 °C [167 and 194 °F].

- All the specimens exposed in the liquid phase showed weight gain before acid cleaning the surface because of scales formed on the surface. Most of the specimens exposed in vapor showed weight loss indicating the occurrence of corrosion.

- At all three temperatures, the general corrosion rates of Type 304B4 were less than 80 nm/yr [0.0032 mil/yr] and those of Type 304B5 were less than 600 nm/yr [0.024 mil/yr]. No clear trend was observed for the influence of temperature on general corrosion rates of each material.

- On average, the general corrosion rates of Type 304B5 were higher than those of Type 304B4.

- The possibility of criticality from the measured corrosion rates and observed pitting seems to be limited in the disposal waste package and in the extended dry storage, because there is only a small amount of moisture present in the waste package or in the canister, and the borated stainless steel consumption by general corrosion and pitting is also limited.

ACKNOWLEDGMENTS

The authors gratefully acknowledge the reviews of Drs. P. Shukla and Y.M. Pan and the editorial review of L. Mulverhill. Appreciation is due to A. Ramos for assistance in the preparation of this paper.

This paper describes work performed by the Center for Nuclear Waste Regulatory Analyses (CNWRA) and its contractors for the U.S. Nuclear Regulatory Commission (USNRC) under Contract No. NRC–02–07–006. The activities reported here were performed on behalf of the USNRC Office of Nuclear Material Safety and Safeguards, Division of High-Level Waste Repository Safety. This paper is an independent product of the CNWRA and does not necessarily reflect the view or regulatory position of the USNRC. The USNRC staff views expressed herein are preliminary and do not constitute a final judgment or determination of the matters addressed or of the acceptability of any licensing action that may be under consideration at USNRC.

REFERENCES

(1) ASTM International, ASTM C1671–07, "Standard Specification for Qualification and Acceptance of Boron Based Metallic Neutron Absorbers for Nuclear Criticality Control for Dry Cask Storage Systems and Transportation Packaging," West Conshohocken, Pennsylvania: ASTM International (2007).

(2) ASTM International, ASTM A887–89, "Standard Specification for Borated Stainless Steel Plate, Sheet, and Strip for Nuclear Application," West Conshohocken, Pennsylvania: ASTM International (2004).

(3) EPRI, "Handbook of Neutron Absorber Materials for Spent Nuclear Fuel Transportation and Storage Applications—2006 Edition," Palo Alto, California: Electric Power Research Institute (2006).

(4) H.J. Goldschmidt, "Effect of Boron Additions to Austenitic Stainless Steels Part II, Solubility of Boron in 18% Cr, 15% Ni Austenitic Steel," *Journal of the Iron and Steel Institute* (1971), p. 910.

(5) K. Wasinger, "High Density Spent Fuel Storage in Spain-Capacity for the Entire Life," *Nuclear Plant Journal* (1993), p. 46.

(6) R.D. McCright, W.G. Halsey, and R.A. Van Konynenburg, "Progress Report on the Results of Testing Advanced Conceptual Design Metal Barrier Materials Under Relevant Environmental Conditions for a Tuff Repository," UCID–21044, Livermore, California: Lawrence Livermore National Laboratory (1987).

(7) J.A. Beavers, N.G. Thompson, and C.L. Durr, NUREG/CR–5709, "Pitting, Galvanic, and Long-Term Corrosion Studies on Candidate Container Alloys for the Tuff Repository," Washington, DC: U.S. Nuclear Regulatory Commission (1992).

(8) J.A. Beavers and C.J. Durr, NUREG/CR–5598, "Immersion Studies on Candidate Container Alloys for the Tuff Repository," Washington, DC: U.S. Nuclear Regulatory Commission (1991).

(9) R.S. Glass, G.E. Overturf, R.E. Garrison, and R.D. McCright, "Electrochemical Determination of the Corrosion Behavior of Candidate Alloys Proposed for Containment of High Level Waste in Tuff," UCID–20174, Livermore, California: Lawrence Livermore National Laboratory (1984).

(10) T.E. Lister, R.E. Mizia, A.W. Erickson, and B.S. Matteson, "General and Localized Corrosion of Borated Stainless Steels," Proceedings of the Corrosion '08 Conference. Paper No. 590, Houston, Texas: NACE International (2008).

(11) T. Lister, R. Mizia, A. Erickson, and S. Birk, "Electrochemical Corrosion Testing of Borated Stainless Steel Alloys," INL/EXT–07–12633, Rev. 1, Idaho Falls, Idaho: Idaho National Laboratory (2007).

(12) T. Lister, R. Mizia, A. Erickson, and Trowbridge, "Electrochemical Corrosion Testing of Neutron Absorber Materials," INL/EXT–06–11772, Rev. 1, Idaho Falls, Idaho: Idaho National Laboratory (2007).

(13) R.A. Van Konynenburg and P.G. Curtis, "Scoping Corrosion Tests on Candidate Waste Package Basket Materials for the Yucca Mountain Project," High Level Radioactive Waste Management, Proceedings of the Seventh Annual International Conference, April 29–May 3, 1996, Warrendale, Pennsylvania: American Nuclear Society (1996), pp. 464–467.

(14) Smith, R.J., G.W. Loomis, C.P. Deltete, "Borated Stainless Steel Application in Spent-Fuel Storage Racks," EPRI TR–100784, Palo Alto, California: Electric Power Research Institute (1992).

(15) H.S. Cole, "Corrosion of Stainless Steel Type 304 Alloyed with Boron or Gadolinium by Plant Process Solutions Containing HNO_3 and HF," ICP–1097, Idaho Falls, Idaho: Idaho National Engineering Laboratory (1976).

(16) D.A. Moreno, B. Molina, C. Ranninger, F. Montero, and J. Izquierdo, "Microstructural Characterization and Pitting Corrosion Behavior of UNS S30466 Borated Stainless Steel," *Corrosion,* Vol. 60 (2004), pp. 573–583.

(17) R.S. Brown, "Corrosion Resistance of Borated Stainless Steels," Wyomissing, Pennsylvania: Carpenter Powder Products (March 1991).

(18) D.V. Fix, J.C. Estill, L.L. Wong, and R.B. Rebak, "General and Localized Corrosion of Austenitic and Borated Stainless Steels in Simulated Concentrated Ground Waters," Vol. 483, Washington, DC: American Society of Mechanical Engineers, Pressure Vessels and Piping Division (2004), pp. 121–130.

(19) X. He, V. Jain, F.P. Bertetti, and D. Pickett, "Evolution of Fluid Chemistry Inside a Waste Package Due to Carbon Steel and Simulated High-Level Waste Glass Corrosion," San Antonio, Texas: CNWRA, (2007).

(20) ASTM International, 2004, ASTM G31–72, "Standard Practice for Laboratory Immersion Corrosion Testing of Metals," West Conshohocken, Pennsylvania: ASTM International (2004).

(21) ASTM International, ASTM G1–03, "Preparing, Cleaning, and Evaluating Corrosion Test Specimens," West Conshohocken, Pennsylvania: ASTM International (2003).

(22) Carpenter Powder Products, "Micro-Melt® NeutroSorb Plus® Alloys Data," Reading, Pennsylvania: CRS Holdings Inc (2003).

(23) X. He, O. Pensado, T. Ahn, and P. Shukla, "Model Abstraction of Stainless Steel Waste Package Degradation," Proceedings of 2011 International High-Level Radioactive Waste Management Conference (IHLRWMC), Albuquerque, New Mexico: American Nuclear Society, April 10–14, 2011, p. 679 (2011).